JACS
JOURNAL OF THE AMERICAN CHEMICAL SOCIETY

COMMUNICATION

pubs.acs.org/JACS

Templated Synthesis of Metal Nanorods in Silica Nanotubes

Chuanbo Gao, Qiao Zhang, Zhenda Lu, and Yadong Yin*

Department of Chemistry, University of California, Riverside, California 92521, United States

Supporting Information

ABSTRACT: We report a general method for the synthesis of noble metal nanorods, including Au, Ag, Pt, and Pd, based on their seeded growth in silica nanotube templates. The controlled growth of the metals occurs exclusively on the seeds inside the silica nanotubes, which act as hard templates to confine the one-dimensional growth of the metal nanorods and define their aspect ratios. This method affords large quantities of noble metal nanorods with well-controlled aspect ratios and high yield, which may find wide use in the fields of nanophotonics, catalysis, sensing, imaging, and biomedicine.

Metal nanorods have received widespread interest due to their unique one-dimensional structure; their consequent unusual optical, electronic, and catalytic properties; and their potential use in chemical sensing, cellular imaging, and therapeutics.[1−3] Specifically, noble metal Au,[4−8] Ag,[9] Pt,[10,11] and Pd[12−15] nanorods have garnered great interest, among which Au nanorods have been most extensively studied due to their plasmonic activity. Most conventional syntheses rely on solution-phase reactions, for example, seed-mediated growth for the synthesis of Au nanorods.[4−8] This synthesis route proves successful in producing Au nanorods with different aspect ratios thereby rendering them with desired properties. However, the general applicability of the method for other metals, the scalability of the reaction, the yield of nanorods relative to byproducts such as spheres, and the sensitivity of the reaction to various parameters (and thus the reproducibility) leave a lot of room for developing alternative approaches for this class of functional materials.[16]

Templating methods have also been pursued to synthesize metal nanorods by employing porous alumina membranes and polycarbonate filtration membranes as hard templates.[17−21] Metal nanorods, typically Au in composition, have been fabricated by using this method via electrochemical deposition and subsequent dissolution of the templates. Typical limitations include the difficulty in controlling both the width and length of the products, low yield because only a monolayer of metal nanorods could be prepared in a membrane template, and the high cost associated with these templates. In general, a practically useful templating method for nanostructure synthesis should meet the following requirements: (1) the convenient availability of well-defined templates in large quantity at low cost; (2) the precise placement of seeds inside the templates; (3) a well-controlled seeded growth process; and (4) a reliable process to selectively remove the templates.

Scheme 1. A General Templating Approach to the Synthesis of Metal Nanorods[a]

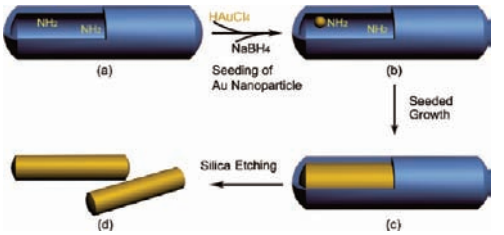

[a] (a) Silica nanotube with amino groups functionalized selectively on the inner surface; (b) Au seed@silica yolk/shell structure; (c) metal nanorod@silica core/shell structure obtained by seeded growth; (d) metal nanorods after etching of silica shells.

Herein, we present a robust templating approach to the synthesis of metal nanorods, including Au, Ag, Pt, and Pd in composition, with well-controlled dimensions and high yield. The success of this method should first be attributed to the employment of silica nanotube templates with tunable dimensions for which a large-scale synthesis was developed recently in our laboratory.[22] Briefly, these high-quality templates were produced by coating uniform nickel-hydrazine rod-like nanocrystals with a layer of silica through a sol−gel process, and then selectively removing the nickel-hydrazine templates to yield tubular structures.

Subsequent templated growth of metal nanorods, as outlined in Scheme 1, involves: (1) the seeding of Au nanoparticles in the cavity of silica nanotubes; (2) the confined growth of metal initiated from the Au seeds, forming a metal nanorod@silica core/shell structure; and (3) the etching of the silica shell producing metal nanorods.

In addition to the synthesis of well-defined templates, introducing Au seeds exclusively into the cavity of these templates is another indispensable step as it ensures that subsequent metal growth occurs in the confined space rather than outside as a result of self-nucleation. There are only a few reports on the seeding of Au nanoparticles in a preexisting nanostructure, which were achieved by infiltration of $HAuCl_4$ solution into the nanostructure followed by reduction by $NaBH_4$.[23,24] In our system, the encapsulated hydrazine inside the silica nanotubes fails in producing Au seeds inside due to their outward diffusion of the templates (Supporting Information (SI)). To produce Au seeds preferentially within the inner cavity, we modified the original silica nanotube synthesis by introducing a layer of 3-aminopropyltriethoxysilane (APS) to the surface of the

Received: October 13, 2011
Published: November 15, 2011

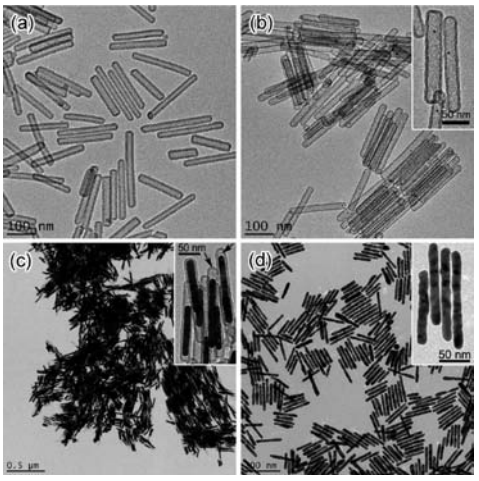

Figure 1. TEM images of the (a) silica nanotubes with inner cavity functionalized with amino groups; (b) Au seed@silica nanotubes; (c) Au nanorod@silica nanotubes after seeded growth; (d) Au nanorods after removal of silica templates.

nickel-hydrazine nanorods before the deposition of a silica layer through the hydrolysis of tetraethyl orthosilicate (TEOS). As is well-known, Au species, including the anionic $AuCl_4^-$ and metallic Au, have a high affinity to amino groups due to electrostatic and/or coordinate interactions. The selective modification of the inner surface of the silica nanotubes with amino groups allows the retention of the Au species inside the templates during the chemical adsorption of $HAuCl_4$, resulting in Au seeds exclusively positioned inside the silica nanotubes after reduction.

Figure 1a shows the TEM image of a typical sample of silica nanotubes, synthesized by using polyoxyethylene(10) cetyl ether (Brij C10) as the surfactant. They possess an average length of 200 nm and a cavity width of 12 nm, which are determined independently by the hydrazine/nickel ratio and the intrinsic size of the surfactant micelles.[22] Modification of the inner surface with amino groups results in no significant change to the tubular morphology of the silica templates. After seeding, Au nanoparticles ~4 nm in size are formed inside each silica nanotube (Figure 1b). No obvious nucleation outside the silica nanotubes has been observed. The UV−vis spectrum of the material (SI) shows an absorption band at ~512 nm, characteristic of small-sized Au nanospheres. To enhance the mass transfer through the silica shell in the following seeded growth of metal nanorods, the Au seed@silica sample was etched with water at 70 °C for 1 h, increasing the pore size in the silica shell,[25] and in the meantime, the inner diameter of the cavity was enlarged to ~15 nm.

The key in the seeded growth step is to maintain a low reaction rate and minimize self-nucleation events. Taking Au for example, we used ascorbic acid as a weaker reducing agent to replace $NaBH_4$ for the reduction of Au salt. However, on direct mixing of the ascorbic acid with $AuCl_4^-$, the solution still quickly turned red, suggesting self-nucleation due to the high reduction potential of $AuCl_4^-$ (+0.93 V vs SHE). To further slow down the self-nucleation, a coordinating ligand, KI, was introduced, which reacts with $AuCl_4^-$ forming a stable complex AuI_4^- with a decreased reduction potential (+0.56 V vs SHE) due to the strong Au−I affinity. An additional capping ligand, typically polyvinylpyrrolidone (PVP), was also added to the growth solution to stabilize the atomic monomer species and further delay the self-nucleation.[26] PVP also has the function of preventing the final products from agglomeration. The as-prepared growth solution, which combines $HAuCl_4$, PVP, KI, and ascorbic acid, remained stable at room temperature for longer than 2 h without obvious self-nucleation, as evidenced by UV−vis spectrophotometry measurements. However, immediately after the Au seed@silica was injected into the growth solution, growth of Au on the existing seeds occurred as evidenced by the color change of the mixture.

The silica nanotube acts as a limiting factor to restrain the growth of metal in one dimension, leading to the formation of nanorods. The seeded growth stops theoretically when the nanorods reach the end of the templates. Figure 1c shows a TEM image of the Au nanorod@silica nanostructures obtained by seeded growth. The final Au nanorods fill the inner space of the silica nanotubes, taking their shape and size. Interestingly, most silica nanotubes are not completely filled by Au nanorods, probably because at the end of the reaction, the concentration of the Au precursors/monomers decreases dramatically, and their limited diffusion to the remaining small free space of the silica nanotubes (indicated by arrows in the inset in Figure 1c) is not able to support extensive continued growth. The low-magnification TEM image in Figure 1c indicates the high yield of the Au nanorods, as no obvious presence of free Au nanospheres has been observed, which could be attributed to the exclusive seeding of the Au nanoparticles inside the silica nanotubes and the high stability of the growth solution against self-nucleation.

Well-defined metal nanorods could be finally obtained after removing the silica shell by NaOH etching. The particular sample of Au nanorods shown in Figure 1d has an average dimension of 17 nm × 150 nm, which is consistent with the cavity size of the silica nanotubes with a slight deviation. The nanorods are uniform in size with high yield, proving the competence of this method in synthesizing high-quality samples.

This method is versatile in affording metal nanorods with different aspect ratios, which can be conveniently achieved by controlling the aspect ratio of the original silica nanotubes through tuning the hydrazine/nickel ratio during the original template synthesis.[22] A series of Au nanorods prepared by this method is presented in Figure 2, showing both the TEM images and the UV−vis−near-IR (NIR) spectra. With the average aspect ratio increasing from 3.5 to 5.7, 14.8, and 21, the longitudinal plasmonic band red-shifts significantly from 755 to 1132, 1885, and 2320 nm, which are close to the values predicted by theoretical calculations ($\lambda_{max} = 95R + 420$ nm; R: aspect ratio).[3] The transverse plasmonic band, on the other hand, blue-shifts from 512 nm (sample a) to ~504 nm (samples b−d) (SI), with the intensity becoming drastically weaker compared with that of the longitudinal bands. The absence of the plasmonic band at 530 nm suggests high yield of nanorods without significant existence of spheres.

The hard-templating method to synthesize metal nanorods is not restricted to Au, but can be readily extended to many other metals, including Ag, Pt, and Pd. Typical samples of Ag, Pt, and Pd nanorods prepared by this method are shown in the TEM images in Figure 3.

Ag nanorods are difficult to synthesize by conventional methods, with only a few reports documented in the literature,[9] but can be easily synthesized using the silica nanotube templates. In preparing the growth solution for Ag nanorods, $AgNO_3$ was used as the metal source, ascorbic acid as the reducing agent, acetonitrile as the coordinating ligand, and sodium citrate as the additional capping ligand. The nitrile group on acetonitrile can

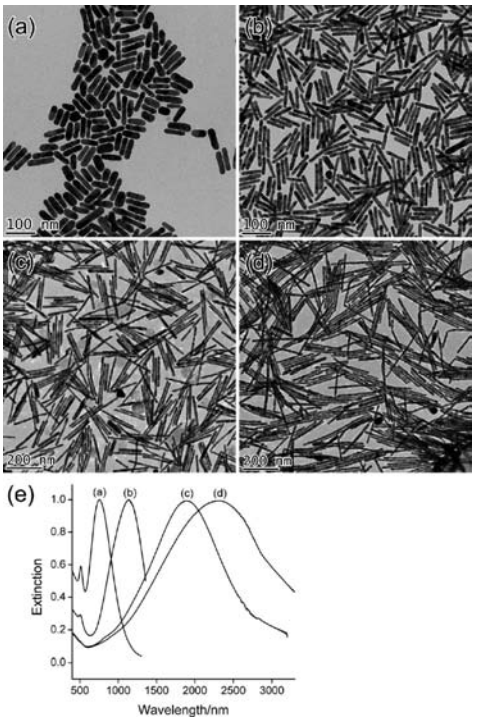

Figure 2. (a–d) TEM images and (e) UV–vis–NIR spectra of Au nanorods prepared by using silica nanotubes with different aspect ratios as templates. Spectra were taken from (a and b) a water solution of the samples, and (c and d) from samples deposited on glass slides.

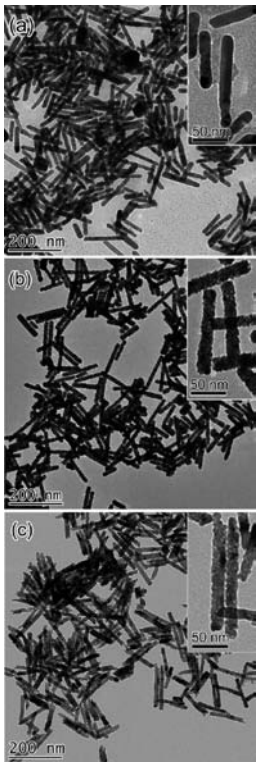

Figure 3. TEM images of (a) Ag, (b) Pt, and (c) Pd nanorods prepared by seeded growth in silica nanotubes.

effectively coordinate to a Ag^+ ion, lowering its reduction potential and thus preventing self-nucleation. The seeded growth of Ag nanorods was initiated by injecting the Au seed@silica into the growth solution. A significant color change was observed, from colorless to yellow, red, blue, gray, and eventually green, indicating a change in the aspect ratio accompanying the growth of the Ag nanorods. The silica shell was removed by etching the sample with NaOH, with a small amount of diethylamine added to the solution to enhance the stability of the Ag nanorods against base etching. Pure Ag nanorods have been obtained by this method, as shown in Figure 3a.

Likewise, to synthesize Pt and Pd nanorods, growth solutions were first prepared, to which the Au seed@silica was injected to trigger seeded growth in the confined space. The growth solution for Pt was prepared with H_2PtCl_6 as the metal source, hydrazine hydrate as the reducing agent, $NaNO_2$ as the coordinating ligand, and PVP as the additional capping ligand. Similarly, the growth solution for Pd contained Na_2PdCl_4 as the metal source, ascorbic acid as the reducing agent, and PVP as the additional capping ligand. TEM images of the Pt and Pd nanorods after etching of silica are displayed in Figure 3b,c, respectively, demonstrating the high yield of the synthesis. The aqueous solutions of the nanorods are black in color, without discernible optical features. By comparing the high-magnification images in the insets, one can easily notice that the Pt and Pd nanorods are grainier than the Au and Ag nanorods, although all are polycrystalline in nature. The cause of the different crystallinity is not clear at the current stage and will be the subject of future investigation.

The seeded growth of metal nanorods in the silica nanotubes has been monitored by TEM and in situ UV–vis–NIR spectrophotometry studies, taking Au and Ag as typical models (Figure 4). Growth intermediates of Au nanorods in silica nanotubes were collected at different growth stages. Prior to quick centrifugation, at each stage additional PVP was added to the growth solution to stabilize the monomer species and effectively stop the growth. The Au seeds in silica nanotubes initially grow isotropically into larger nanospheres. After reaching the diameter of the silica nanotubes, they begin growing one-dimensionally as a result of the confinement of the silica shell, forming anisotropic nanorods which continue growing in the longitudinal direction of the silica nanotube until reaching or near to the ends of the silica nanotubes. It is worth noting that the anisotropic growth occurs mainly from a single seed rather than the multiple seeds contained in each nanotube, mainly because the growth of one seed decreases the precursor concentration in the surrounding and prohibits the extensive growth of the adjacent seeds.

The growth of Au nanorods in the silica nanotubes is accompanied by a change in the optical property, as shown in Figure 4b. Shortly after the growth started, a single absorption peak at ~530 nm was observed, indicative of the formation of Au nanospheres. As the growth went on, a longitudinal plasmon band of Au at a longer wavelength appeared, suggesting the formation of Au nanorods. The longitudinal band red-shifted thereafter, accompanied by a blue-shift of the transverse band, consistent with an increase in the aspect ratio of the nanorods resulting from an elongation of the Au nanorods. The extinction increases throughout the process, due to an increase in the absolute amount of elemental Au. These results match very well with the TEM observations and confirm the growth process of Au nanorods in silica nanotubes. Similar evolution of the plasmon resonance peaks was also observed for Ag nanorods, as shown in Figure 4c, confirming the same seeded growth mechanism. Apparently, harvesting the samples at different

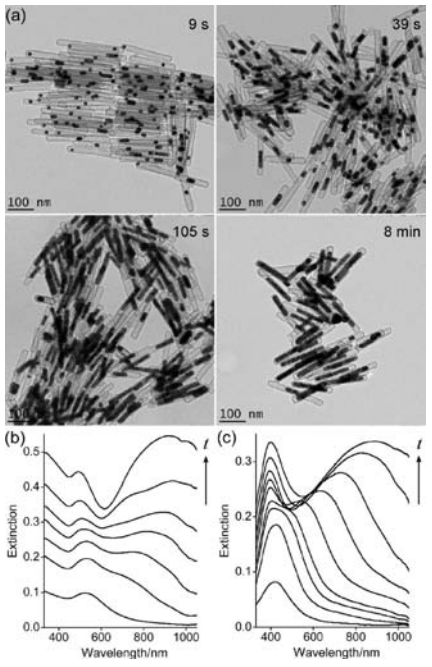

Figure 4. (a) Growth intermediates of Au nanorods in silica nanotubes, observed by TEM. (b–c) Evolution of plasmonic peaks during the seeded growth of Au (b, reaction time t = 9, 21, 30, 39, 48, 66, and 105 s in order) and Ag (b, t = 1.2, 2.7, 3.7, 4.3, 6, 8.3, 11.3, 17, and 22.3 min in order) nanorods in the silica nanotubes, as monitored by in situ UV–vis–NIR spectrophotometry.

reaction stages followed by template removal represents another effective method to control the aspect ratio of metal nanorods.

In summary, we have presented a general method to synthesize noble metal nanorods in silica nanotubes, which includes Au seeding in the cavity of the silica nanotubes, seeded growth of metal nanorods in the confined space, and removal of the silica templates by chemical etching. This robust templating process is highly scalable as the silica nanotubular templates can be obtained in large quantities at low costs. The unique seeding process affords metal nanorods with high yield by exclusively positioning the Au seeds inside the silica nanotubes. The growth solutions combining a metal source, a reducing agent, a coordinating ligand, and an additional capping ligand remain highly stable until the addition of seeds, allowing preferential growth on the seeds without homogeneous nucleation. The convenient availability of silica nanotube templates with different dimensions also affords metal nanorods with well-controlled aspect ratios. The wide applicability of this method to the synthesis of noble metal nanorods of various compositions, which were previously difficult to fabricate with high quality and in large quantity, opens up great opportunities for discovering new properties and designing novel materials for diverse future applications.

■ ASSOCIATED CONTENT

Supporting Information. Details of experimental procedures, additional UV–vis–NIR spectra, control experiments, and multimedia on the seeded growth of metals in silica nanotubes (avi). This material is available free of charge via the Internet at http://pubs.acs.org.

■ AUTHOR INFORMATION

Corresponding Author
yadong.yin@ucr.edu

■ ACKNOWLEDGMENT

Financial support of this work was provided by U.S. Department of Energy (DE-SC0002247) and the National Science Foundation (DMR-0956081). Y.Y. thanks the Research Corporation for Science Advancement for the Cottrell Scholar Award, 3M for the Nontenured Faculty Grant, and DuPont for the Young Professor Grant. We also thank the Central Facility for Advanced Microscopy and Microanalysis at UCR for access to TEM analysis.

■ REFERENCES

(1) Pérez-Juste, J.; Pastoriza-Santos, I.; Liz-Marzán, L. M.; Mulvaney, P. *Coord. Chem. Rev.* **2005**, *249*, 1870.
(2) Murphy, C. J.; Gole, A. M.; Stone, J. W.; Sisco, P. N.; Alkilany, A. M.; Goldsmith, E. C.; Baxter, S. C. *Acc. Chem. Res.* **2008**, *41*, 1721.
(3) Huang, X.; Neretina, S.; El-Sayed, M. A. *Adv. Mater.* **2009**, *21*, 4880.
(4) Jana, N. R.; Gearheart, L.; Murphy, C. J. *Adv. Mater.* **2001**, *13*, 1389.
(5) Nikoobakht, B.; El-Sayed, M. A. *Chem. Mater.* **2003**, *15*, 1957.
(6) Gole, A.; Murphy, C. J. *Chem. Mater.* **2004**, *16*, 3633.
(7) Sau, T. K.; Murphy, C. J. *Langmuir* **2004**, *20*, 6414.
(8) Kou, X.; Zhang, S.; Tsung, C.-K.; Yang, Z.; Yeung, M. H.; Stucky, G. D.; Sun, L.; Wang, J.; Yan, C. *Chem.—Eur. J.* **2007**, *13*, 2929.
(9) Zhang, J.; Langille, M. R.; Mirkin, C. A. *Nano Lett.* **2011**, *11*, 2495.
(10) Krishnaswamy, R.; Remita, H.; Impéror-Clerc, M.; Even, C.; Davidson, P.; Pansu, B. *ChemPhysChem* **2006**, *7*, 1510.
(11) Peng, Z.; Yang, H. *Nano Today* **2009**, *4*, 143.
(12) Xiong, Y.; Cai, H.; Yin, Y.; Xia, Y. *Chem. Phys. Lett.* **2007**, *440*, 273.
(13) Xiong, Y.; Cai, H.; Wiley, B. J.; Wang, J.; Kim, M. J.; Xia, Y. *J. Am. Chem. Soc.* **2007**, *129*, 3665.
(14) Lim, B.; Jiang, M.; Tao, J.; Camargo, P. H. C.; Zhu, Y.; Xia, Y. *Adv. Funct. Mater.* **2009**, *19*, 189.
(15) Chen, Y.-H.; Hung, H.-H.; Huang, M. H. *J. Am. Chem. Soc.* **2009**, *131*, 9114.
(16) Millstone, J. E.; Wei, W.; Jones, M. R.; Yoo, H.; Mirkin, C. A. *Nano Lett.* **2008**, *8*, 2526.
(17) Kyotani, T.; Tsai, L.-f.; Tomita, A. *Chem. Commun.* **1997**, 701.
(18) van der Zande, B. M. I.; Böhmer, M. R.; Fokkink, L. G. J.; Schönenberger, C. *J. Phys. Chem. B* **1997**, *101*, 852.
(19) Cepak, V. M.; Martin, C. R. *J. Phys. Chem. B* **1998**, *102*, 9985.
(20) Martin, B. R.; Dermody, D. J.; Reiss, B. D.; Fang, M.; Lyon, L. A.; Natan, M. J.; Mallouk, T. E. *Adv. Mater.* **1999**, *11*, 1021.
(21) van der Zande, B. M. I.; Böhmer, M. R.; Fokkink, L. G. J.; Schönenberger, C. *Langmuir* **1999**, *16*, 451.
(22) Gao, C.; Lu, Z.; Yin, Y. *Langmuir* **2011**, *27*, 12201.
(23) Yuan, C.; Luo, W.; Zhong, L.; Deng, H.; Liu, J.; Xu, Y.; Dai, L. *Angew. Chem., Int. Ed.* **2011**, *50*, 3515.
(24) Liu, B.; Zhang, W.; Feng, H.; Yang, X. *Chem. Commun.* **2011**, *47*, 11727.
(25) Hu, Y.; Zhang, Q.; Goebl, J.; Zhang, T.; Yin, Y. *Phys. Chem. Chem. Phys.* **2010**, 11836.
(26) Yin, Y.; Alivisatos, A. P. *Nature* **2005**, *437*, 664.